Mechanical Properties and Nanostructure Correlation of Condensation-Type Poly(dimethyl siloxane)/Layered Silicate Hybrids

S. P. Vasilakos, P. A. Tarantili

National Technical University of Athens, School of Chemical Engineering, Polymer Technology Lab. 9, Heroon Polyrechniou str., Zographou, GR 15780, Athens, Greece

Received 11 August 2011; accepted 12 November 2011
DOI 10.1002/app.36479
Published online 1 February 2012 in Wiley Online Library (wileyonlinelibrary.com).

ABSTRACT: Composites of silicone rubber reinforced with organomontmorillonite (OMMT) nanoparticles were prepared by direct mixing and characterized in terms of morphology, in correlation with mechanical performance. Two grades of commercial montmorillonite (MMT) with different types of organic modification were studied, namely Cloisite® 20A and Cloisite® 30B. Low, medium, and higher molecular weight PDMS were used as matrices. Using X-ray diffraction analysis, it was shown that OMMT loadings at a weight ratio to resin ranging from 5 to 10 parts per hundred (phr) can produce delamination hybrids. Mechanical testing showed that for OMMT loadings up to 8 phr, the prepared nanocomposites present higher tensile strength, stiffness, and tear resistance with respect to the neat silicone. Improvement of the solvent resistance was also recorded by swelling experiments in toluene, and this behavior of the nanocomposites is consistent with their mechanical properties. The results showed that processing characteristics, as well as the overall reinforcing efficiency of nanofillers, are greatly dependent on the initial molecular weight of the elastomer, because this parameter controls the resulting network density and concentration of polar end groups. The content of organic modification of MMT was also found as an important characteristic for proper filler dispersion. © 2012 Wiley Periodicals, Inc. J Appl Polym Sci 125: E548–E560, 2012

Key words: polysiloxanes; nanocomposites; organoclay; mechanical properties; structure-property relations

INTRODUCTION

Poly(dimethylsiloxane) (PDMS) is useful in a variety of applications including those in medical, electronic, automotive, and aerospace industries. However, silicone polymers are characterized by poor mechanical properties, and, therefore, reinforcing fillers must be added to overcome this drawback. PDMS is commonly reinforced by fumed silica at significant concentrations to form high-performance composites. The use of such large amounts of silica significantly increases the opacity of the resulting materials as well as their specific weight. Alternatively, fillers with large specific area and aspect ratio, such clay nanoplatelets, could bring better mechanical performance, improved barrier properties and thermal stability, keeping the material transparent and lightweight. In spite of their similarities in structure, montmorillonite (MMT) does not naturally delaminate in PDMS matrix. To achieve the expected properties of nanocomposites, stacked clay platelets must be dispersed, and strong interactions between the polymer and mineral phase must be promoted. Because of its hydrophilic nature, clay is generally modified by quaternary ammonium surfactants to increase the intergallery spacing and to achieve enough hydrophobicity, which will readily promote miscibility with the polymer matrix.

Successful treatments of the reinforcement include that of Burnside and Giannelis,[1] who studied PDMS/organomontmorillonite (OMMT) nanocomposite systems, using melt intercalation. The organosilicate was prepared by ion exchanging Na^+-MMT with dimethyl ditallow ammonium bromide. The prepared nanocomposites exhibit decreased solvent uptake and increased thermal stability.

In another work, organosilicate was also prepared by ion-exchange Na^+-MMT with hexadecyltrimethylammonium bromide, and the silicone rubber/OMMT hybrids were prepared by simple mechanical mixing.[2] It was observed that the mechanical properties and thermal stability of hybrids were very close to those of aerosilica-filled silicone rubber.

A novel kind of OMMT was successfully prepared by Wang et al.[3,4] who used *N,N*-di(2-hydroxyethyl)-*N*-dodecyl-*N*-methylammonium chloride as intercalation agent. Exfoliated nanocomposites were prepared using addition-type silicone rubber via solution intercalation. The enhanced mechanical and physical properties demonstrated the efficient reinforcing and

Correspondence to: P. A. Tarantili (taran@chemeng.ntua.gr).

improved thermal stability achieved by the incorporation of OMMT.

In a more recent work, Kim et al.[5] used bis(3-triethoxysilylpropyl)tetrasulfide to functionalize two commercially available clays, namely sodium MMT and Cloisite® 25A. Incorporation of the tetrasulfide group-containing clays was found to be effective for the enhancement of interfacial interaction between PDMS and clay, by possible chemical reaction of tetrasulfide groups with vinyl-terminated PDMS. According to the results obtained by swelling in toluene, the crosslinking density was lower than that of neat PDMS, indicating that the observed improvement in mechanical properties arises from enhanced compatibility between the constituents and not from the increase of crosslinking density.

PDMS/clay nanocomposites have also been produced by Labruyère et al.[6,7] by the use of ω-ammonium functionalized oligo-PDMS surfactant [PDMS-$N^+(CH_3)_3$]. The clay treated with PDMS-$N^+(CH_3)_3$ has been compared to nanocompositions prepared with PDMS containing nonexchanged sodium MMT as well as two types of organoclay modified by using either alkyl ammonium cations ($C_{38}H_{80}N^+$) and hydroxyalkyl ammonium ($C_{22}H_{48}ON^+$) cations. It was observed that nanocomposites based on PDMS-$N^+(CH_3)_3$ exhibit the best filler dispersion and significantly higher viscosity, due to better intercalation of PDMS chains into clay galleries. Increase of stiffness with increasing the content of treated clay in PDMS was also recorded, but no significant differences between the different organo-modifiers were detected. Regarding the transport properties for organic vapors, sorption is not influenced by the presence of organomodified clay, whereas the diffusion parameter is significantly affected, within the range of sorbed vapor 0–4% for acetone and 0–7% for *n*-hexane.[7]

With respect to the characteristics of the elastomeric matrix, recent studies tried to investigate the related effects. Takeuchi and Cohen[8] published on systems of OMMT and PDMS networks prepared from hydroxyl- or vinyl-terminated precursors. No improvement in the Young's modulus of networks synthesized from vinyl-terminated precursors was obtained. The above authors concluded that enhancement of the modulus was obtained only for nonoptimal networks formed with hydroxyl-terminated precursor chains in contrast to vinyl-terminated chains. Their results indicate that reinforcing effect of these elastomers can be attributed to an anchorage of hydroxyl end group to the silicate filler, which dramatically reduces the soluble fraction and binds pendent chain ends.

The preparation procedure is also very critical for proper filler dispersion. Bokobza[9] made a series of silicone/nanoclay composites from organically modified MMT and addition-type PDMS. Nanoclay platelets were mixed with hydride-terminated PDMS and subsequently cross-linked by 1,3,5,7-tetravynil-1,3,5,7-tetramethylcyclotetrasiloxane via a chemical reaction catalyzed by platinum divinyltetramethylsiloxane. However, the process demands cure time of 12 h, making impractical the application of this method for continuous molding processes. Moreover, only minor improvements in tensile properties were reported. A new strategy to prepare disorderly PDMS nanocomposites was developed by Ma et al.[10] More specifically, a quarternary ammonium-containing polysiloxane surfactant was adopted to modify the clay. The slurry of modified clay was then mixed with commercial RTV silicone rubber by hand, and exfoliation was achieved, as confirmed by TEM and XRD analysis. The resulting silicone/nanoclay composites presented significant improvement of their mechanical properties.

To overcome difficulties related with the preparation of high-temperature vulcanized silicone rubber (HTV-SR) nanocomposites, Wang and Chen[11] prepared a master batch of the above-modified MMT (OMMT-MB) by solution intercalation.

Masterbatches of MMT and OMMT with siloxane-polyether surfactant were used for the preparation of high-molar mass PDMS-gum nanocomposites.[12] The incorporation of 5 phr OMMT into PDMS matrix, via masterbatch compounding, improved the tensile strength as much as that obtained with composites loaded with 3 phr OMMT clay by direct addition of the clay to PDMS.

HTV-SR/OMMT-MB-20% nanocomposites demonstrate enhanced tensile and thermal properties in comparison with HTV-SR/OMMT-20%. In a recent work,[13] this type of hyperbranched OMMT was directly added to a HTV-SR system. The enhanced tensile properties suggest an efficient reinforcing agent because of the good dispersion of nanosilicate layers and the resulting "anchoring" effect of the hyperbranched macromolecules in the composite. An alternative technique was proposed by Horsch et al.,[14] who used supercritical carbon dioxide ($scCO_2$) to delaminate dry clays, and found that the extent of dispersion is dependent on the CO_2-philicity of the nanoclay. In addition, natural clay was partially dispersed with $scCO_2$, using a CO_2-philic PDMS matrix.

From the study of a multisystem, it has been shown that for nanocomposites based on silanol-terminated PDMS and alkylammonium-modified layered-silicate fillers, there are two factors controlling silicate dispersion: (i) the presence of the appropriate number of long ammonium-bound alkyl chains and (ii) the presence of the appropriate number of polar functional groups. Therefore, dispersion is not a function of molecular weight or viscosity, but it is

TABLE I
Main Characteristics of the Nanoclays Used in This Work

	Cloisite 30B	Cloisite 20A
Organic modifier	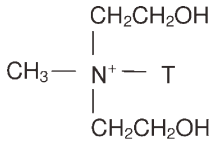	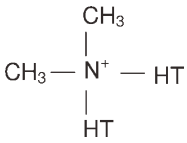
	Methyl, tallow, bis-2-hydroxylethyl, and quaternary ammonium	Dimethyl, dihydrogenated tallow, and quaternary ammonium
Modifier concentration	90 meq/100 g clay	95 meq/100 g clay
Weight loss in ignition	30%	38%

Where HT is hydrogenated tallow (~65% C18, ~30% C16, and ~5% C14) and T is tallow (~65% C18, ~30% C16, and ~5% C14).

rather influenced by the concentration of silanol end-groups.[15]

In an attempt to correlate silicate dispersion with the resulting mechanical properties in the PDMS/layered silicate nanocomposites, a systematic study was performed of the mechanical properties, equilibrium swelling, and sol fraction measurements of cross-linked silanol-terminated PDMS networks, as a function of the type and content of nanofiller as well as of the composition of base resin.[16] In MMT systems, in particular, it was observed that equilibrium solvent uptake and mechanical properties are independent of dispersion state, which suggest that edge interactions play a more significant role than the degree of exfoliation.

Although many parameters have been considered so far, regarding the type and treatments of nanofillers as well as the preparation processes with respect to the final structure and properties of nanocomposites, there is not enough literature related to the effect of the initial molecular weight of silicone and, more specifically, data correlating the anticipated network characteristics with reinforcing efficiency of clays. In fact, molecular weight might be a critical parameter, not only because of variations in rheological parameters, but also due to the different chemistry of the systems (e.g., concentration of —OH end groups). Consequently, cross-linking reactions and network formation may vary according to the initial molecular weight of the matrix. Based on the above, the effect of the type of organic modification and the molecular weight of PDMS on the structure and properties of nanocomposites was evaluated in this work. OMMT composites with hydroxyl-terminated PDMS were prepared by sonication at room temperature. The composites were characterized using X-ray diffraction (XRD). In addition, their tensile and tear properties as well as the solvent uptake were studied, and interpretation of the obtained results based on the structural parameters of nanocomposites was proposed.

MATERIALS AND METHODS

Materials

Silanol-terminated PDMS—grades DMS-S31, DMS-S35, and DMS-S42 (Gelest Inc.) of low (LMW: 26,000 g/mol), medium (MMW: 49,000 g/mol), and higher (HMW: 77,000 g/mol) molecular weight, respectively—were the silicon base elastomers used in this work. The vulcanization reaction system was tetrapropoxysilane (Aldrich) as a cross-linker and dibutyl tin dilaurate (Aldrich) as catalyst. Commercial MMT clays under the trade name Cloisite® 30B and Cloisite® 20A, supplied by Rockwood Clay Additives GmbH, were also used as reinforcing nanofiller. The main characteristics are presented in Table I.

Methods

Blending of clay/PDMS composites

Efficient dispersion of nanoparticles was achieved by sonicating with an ultrasound probe, the PDMS, and the appropriate amount of clay for 6 min at room temperature. The cross-linking system was then added and dispersed into the mixture, and the samples were cast into molds for subsequent cure at room temperature for 12 h.

X-ray diffractometer

XRD of clay and PDMS nanocomposites, in order to evaluate the evolution of the clay d_{001} reflection, was performed in a Siemens 5000 (35 kV and 25 Ma) using Cu Kα X-ray radiation with a wavelength of $\lambda = 0.154$ nm. The diffractograms were scanned in the 2θ range from 2° to 10°, with a rate of 2°/min.

Samples for X-ray analysis were obtained from cast sheets to avoid any preferred orientation of the clay.

Mechanical tests

Indentation hardness was determined with a Shore A durometer on 25 × 25 × 10 mm samples according to ASTM specification D 2240. The Shore A durometer was held in a vertical position, and the pressor foot was applied parallel to the surface of the sample. Ten readings were taken with a 6-mm distance maintained among them.

Tensile tests were carried out according to ASTM D 412 specification in an Instron tensometer (model 4466), equipped with a load cell of maximum capacity of 10 kN, operating at grip separation speed 100 mm/min. All measurements were run at 25°C. Tear tests were conducted on a UTM testing machine, model AEGIS 1000. The rate of extension was 100 mm/min, the thickness of specimen was 0.55 mm, and five specimens from each composition were tested.

Swelling experiments

The solvent uptake of immersed PDMS nanocomposite samples was also measured at 25°C. Preweighed samples were immersed in toluene, and, at different time intervals, the swollen samples were removed, rapidly blotted, and reweighed to minimize evaporation of the absorbed toluene. This procedure was continued for a few days, and the final weight of swollen samples at the equilibrium state was recorded. For each sample, three specimens were tested, and the average was calculated.

Based on measurements of samples weight in equilibrium swollen state, the polymer volume fraction in the swollen network (u_2) was calculated by the following equation:

$$u_2 = \frac{V_{\text{dry}} - V_{\text{filler}}}{V_{\text{swollen}} - V_{\text{filler}}} = \frac{M_p/\rho_p - M_f/\rho_f}{M_p/\rho_p + M_s/\rho_s - M_f/\rho_f} \quad (1)$$

where V_{dry} is the volume of dry polymer, V_{filler} is the volume of the nanofiller (considering the inorganic component without coating), V_{swollen} is the volume of the swollen sample at equilibrium, M_p, M_f, and M_s are the weight of polymer, filler, and solvent, respectively, and ρ_p, ρ_f, and ρ_s are the density of polymer, filler, and solvent, respectively.

M_c calculation

The average molar mass between cross-linking points (M_c) was calculated using the classic Flory–Rehner equation assuming an ideal polymer network without fillers. The above theory provides the following relationship between polymer volume fraction and molecular weight between cross-links in a swollen polymer network:

$$\rho/M_C = -[\ln(1-u_2) + u_2 + \chi u_2^2]/Vu_2^{1/3} \quad (2)$$

where ρ is the density of the polymer network, M_c is the average molar mass between cross-linking points, u_2 is the polymer volume fraction in the swollen network, χ is the Flory–Huggins polymer–solvent interaction parameter, and V is the molar volume of the swelling solvent.

Micromechanical modeling

Numerous attempts have been made for modeling the properties of nanocomposites and correlation of the experimental data with the deriving models. In this work, the Halpin–Tsai equations were adopted as a means to predict tensile modulus as a function of the morphology of MMT/PDMS nanocomposites.[17]

This model assumes that the particles are aligned with loading direction and gives the modulus of the composite as a function of the modulus of polymer and that of the particles, but also as a function of the aspect ratio by the inclusion of a shape factor. The expression for the longitudinal tensile modulus is given by

$$\frac{E_{11}}{E_m} = \frac{1 + 2(L/t)f_p\eta}{1 - f_p\eta} \quad (3)$$

where f_p is the particle volume fraction, L is the length, t is the thickness of the dispersed clay particle, E_p is the effective particle modulus, E_m is the matrix modulus, E_{11} is the longitudinal stiffness, and η is given by

$$\eta = \frac{(E_p/E_m) - 1}{(E_p/E_m) + 2(L/t)} \quad (4)$$

With the conventional miscible composite, where the polymer is unable to penetrate into the space between clay layers, the particle volume fraction (f_p) can be calculated from the weight fraction through the equation:

$$f_p = \frac{W_p/\rho_p}{W_p/\rho_p + (1 - W_p)/\rho_m} \quad (5)$$

where W_p is the particle weight fraction and ρ_p and ρ_m are the clay particle density and the matrix density, respectively.

The morphology of polymer/layered-silicate composites has a hierarchical structure. The dispersion of the clay in the matrix is typically described in

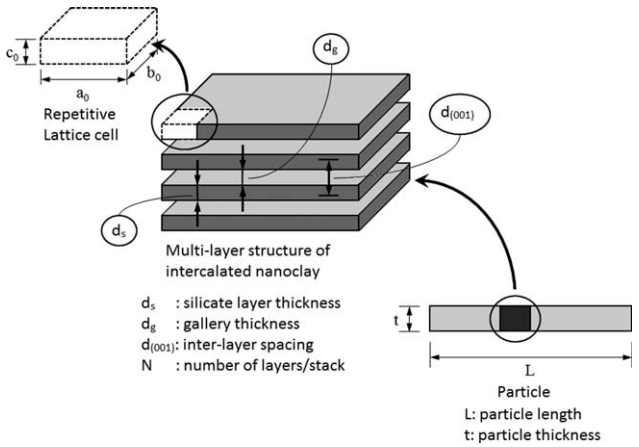

Figure 1 Hierarhical structure of the nanoclay.[18]

terms of intercalation versus exfoliation. In the intercalated structure, a significant number of chains are inserted into the galleries, and the interlayer spacing is correspondingly expanded. The fully exfoliated morphology consists of single silicate layers dispersed in a polymer matrix. In the case of intercalated clay nanocomposites, the filler particles are idealized as a multilayer stack containing N single silicate sheets (each sheet has an area A, an effective thickness d_s, and mass M) with uniform interlayer spacing $d_{(001)}$, as shown in Figure 1.[18] The particle thickness t can be related with the internal structural parameters N and $d_{(001)}$ through:

$$t = (N-1)d_{(001)} + d_s \tag{6}$$

Each individual silicate sheet further consists of repetitive lattice cells, each of area A_0, thickness d_s, and molecular weight M_0. Based on this approach, the particle contains silicate sheets as well as interlayer galleries, and the particle weight fraction W_p differs from clay weight fraction W_c. These quantities are related in terms of the following equation[18]:

$$\frac{W_p}{W_c} = \frac{\rho_p V_\rho}{\rho_{\text{silicate}} V_{\text{silicate}}} = \left(\frac{\rho_p}{\rho_{\text{silicate}}}\right) / \left(\frac{V_{\text{silicate}}}{V_p}\right) = \frac{\rho_p}{\rho_{\text{silicate}}}\frac{1}{\chi} = \alpha \tag{7}$$

where χ is the volume fraction of silicate in the effective particle and ρ_{silicate} is the density of the silicate sheet. The volume fraction can be calculated according:

$$\chi = \frac{V_{\text{silicate}}}{V_p} = \frac{Nd_s}{(N-1)d_{(001)} + d_s} \tag{8}$$

where V_{silicate} and V_p are the volumes assigned to the silicate sheets in a stack and to the effective particle, respectively.

From eq. (7), eq. (5) becomes

$$f_p = \frac{W_c/\rho_p}{W_c/\rho_p + \left(\frac{1}{a} - W_c\right)/\rho_m} \tag{9}$$

When W_c is small, as it often is for the nanocomposite, eq. (9) can be linearized as follows:

$$f_p \cong \left(\frac{\rho_m}{\rho_{\text{silicate}}}\frac{1}{\chi}\right) W_c \tag{10}$$

The density ρ_{silicate} can be calculated from the MMT lattice parameters:

$$\rho_{\text{silicate}} = \rho_{\text{lattice}} = \frac{M_0}{A_0 d_s} = \frac{2.44}{d_s}\text{nm}\cdot\text{g/cm}^3 \tag{11}$$

where $M_0 = 720$ g/mol is the molecular weight and $A_0 = a_0 b_0 = 0.53 \times 0.92$ nm^2 $= 0.49$ nm^2 the planar area of the lattice, respectively.[18]

To calculate η, the following terms were determined:

$$\frac{E_p}{E_m} = \frac{Nd_s E_{\text{silicate}}}{tE_m} \tag{12}$$

$$\frac{L}{t} = \frac{\text{L}}{(N-1)d_{(001)} + d_s} \tag{13}$$

Based on the above model, there is a morphological transition from complete exfoliation ($N = 1$) to intercalation $N \geq 2$.

In this study, commercial MMTs (Cloisite 30B and Cloisite 20A) were used as reinforcement of PDMS elastomeric matrix. According to the literature and manufacture's data, $d_s = 1.4$ nm,[19,20] $E_{\text{silicate}} = 176$ GPa,[21] and L = 50–100 nm (in exfoliated structures).[19]

RESULTS AND DISCUSSION

X-ray diffraction analysis

The X-ray diffraction (XRD) pattern of Cloisite 30B and Cloisite 20A shows a diffraction peak at 2θ values of 4.88° and 3.93°, respectively. A series of XRD patterns of low and high-molecular PDMS composites, containing various OMMT loadings, are presented in Figures 2 and 3. The featureless patterns of low-molecular weight PDMS hybrids for 2 phr Cloisite 30B (Fig. 2) and for those of Cloisite 20A (Fig. 3) in the range 2–5 phr suggest that mixed exfoliated/intercalated structures were formed. Generally, the driving force into clay galleries results from the enthalpic contribution related to the establishment of many favorable polar polymer–surface interactions.[22] On the other hand, it is reasonable that —OH-

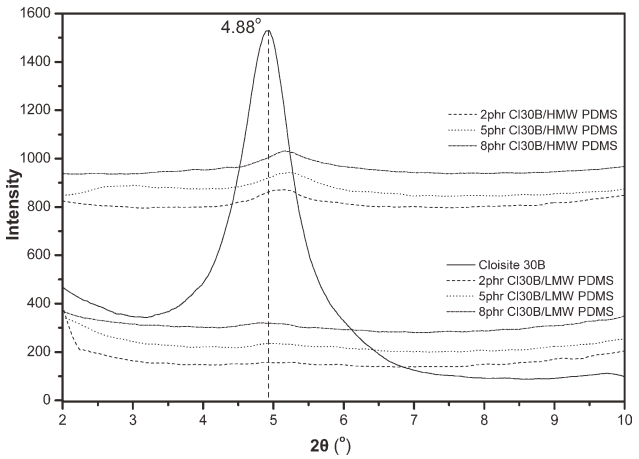

Figure 2 XRD spectra of Cloisite® 30B/PDMS nanocomposites.

terminated groups interact with organic surfactant, thus facilitating filler exfoliation, and, therefore, the hydrophobicity of the organic surfactant could also be essential for a good dispersion. In the case of Cloisite 30B, the hydroxyl groups of organic surfactant may interact with the hydroxyl end groups of PDMS and facilitate intercalation of clay platelets by the elastomer molecules.

These results are in agreement with those of Kim et al.,[23] who studied condensation PDMS nanocomposites containing Cloisite 30B as reinforcement. According to their XRD spectra, fully dispersed structures were achieved at a content of 2 phr OMMT, and this structure was further confirmed by TEM.

On the other hand, Cloisite 20A is characterized by relatively high content of organic modifier and high-intergallery spacing, which facilitates the intercalation process by PDMS molecules.

From Figures 2 and 3, it can also be observed that the angle of pure MMT shifted to lower values for HMW PDMS nanocomposites loaded with 2–8 phr Cloisite 30B and Cloisite 20A. In PDMS hybrids with clay loadings ranging from 5 to 8 phr, clear peaks were observed in XRD patterns for both types of clay, which corresponds to partially intercalated/exfoliated nanocomposite structures.

Comparing the three PDMS systems studied in this work, it is obvious that low-molecular PDMS elastomer gave good dispersion, especially at low-clay loadings. The enhanced mobility of low-molecular weight molecules facilitates their penetration into clay galleries, thus producing intercalated and exfoliated structures. In addition, a relationship between vulcanization time of PDMS, being proportional with restriction of chain mobility as cross-linking density progressively increases, and the intercalation process of clay reinforcement was established. It was observed that high-molecular weight PDMS gives shorter curing time than that recorded for low-molecular weight elastomer, which was attributed to the fact that in the higher molecular weight PDMS system, the concentration of hydroxyl end groups that participate in the condensation curing reaction is lower, and, therefore, the system solidifies within a short time period in comparison with the time required for low-molecular weight systems. Therefore, it seems that there was not sufficient time for the elastomer chains to penetrate into the silicate layers and exfoliate the structure of OMMT. As a result, the intensity of the obtained XRD peaks increases with increasing molecular weight of the matrix, which is an indication for limited exfoliation taking place in higher molecular weight PDMS matrix nanocomposites.

These results are in agreement with those appeared in the literature. Studies on PDMS/fluoroectorite systems by LeBaron and Pinnavaia[24] revealed the effect of parameters, such as polarity match among the linear polymer, gallery surface, and gallery cation of nanoclay, on the intercalation process of PDMS molecules.

The molecular weight of condensation PDMS plays a significant role on the efficiency of MMT dispersion. An even more critical factor is reported the concentration of end groups, particularly the polar end groups.[15] By increasing the concentration of groups, such as amines and silanols, enhanced compatibility can be detected in contrast to the nonpolar groups, such as vinyl and hydrides.

Mechanical performance of OMMT/PDMS nanocomposites

To explore the interrelation of nanocomposite structure with materials performance, characterization with different techniques was carried out. Durometer hardness (Shore A) data as a function of clay loadings are presented in Table II. It is clear that unloaded low-molecular PDMS shows higher hardness values in comparison with high-molecular

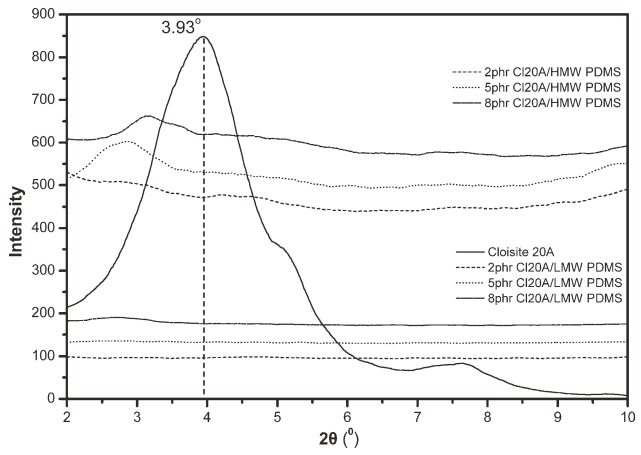

Figure 3 XRD spectra of Cloisite® 20A/PDMS nanocomposites.

TABLE II
Hardness Results of OMMT/PDMS Nanocomposites

Clay content (phr)	LMW PDMS		MMW PDMS		HMW PDMS	
	Cloisite 30B	Cloisite 20A	Cloisite 30B	Cloisite 20A	Cloisite 30B	Cloisite 20A
0	49.6 ±1.3		45.7 ±1.9		39.1 ±1.2	
1	50.2 ±1.7	49.7 ±1.9	46.4 ±1.4	46.7 ±1.9	41.3 ±2.7	44.9 ±1.5
2	50.8 ±1.4	52.3 ±1.6	47.7 ±1.2	49.2 ±2.1	41.6 ±1.7	43.2 ±1.4
3.5	51.4 ±1.3	52.9 ±1.2	48.5 ±1.7	50.2 ±1.3	41.4 ±1.8	45.7 ±0.8
5	54.1 ±1.8	55.1 ±1.9	50.5 ±1.1	51.1 ±0.7	44.2 ±1.6	46.5 ±1.8
8	58.4 ±1.2	59.2 ±1.9	52.1 ±2.0	53.3 ±1.1	47.0 ±1.8	47.6 ±1.6
10	58.0 ±1.6	62.3 ±0.9	52.7 ±1.1	58.3 ±1.3	44.8 ±1.8	53.1 ±2.2

weight systems, and this effect can also be observed for their nanocomposites. The increased hardness of low-molecular weight systems can be due to the higher degree of cross-linking for these elastomers, leading eventually to higher network density. Cloisite 20A is more efficient for the increase of hardness, especially at 10 phr loading into PDMS matrix, due to more efficient dispersion of this type of reinforcement within the PDMS matrix and the intercalation of PDMS molecules along the Cloisite 20A silicate layers (as it was conformed with XRD results).

The tensile properties of PDMS hybrids were also studied, and the tensile strength results are presented in Figure 4. It can be seen that tensile strength of LMW polysiloxane is improved by the incorporation of the examined types of clay reinforcement. The incorporation of Cloisite 20A showed higher reinforcing efficiency for PDMS in comparison with Cloisite 30B. This can be probably due to stronger interfacial interactions, such as physical absorption, hydrogen bonding, dipole interactions, or even chemical reactions, between polymer chains and nanoparticles of Cloisite 20A. Therefore, the advantage of higher intergallery spacing of this grade of nanoclay might be further enhanced by the above interactions leading to more efficient intercalation and to improved reinforcing effect.

The increase of clay loading does not significantly affect tensile characteristics of Cloisite 30B/PDMS hybrids. However, a maximum for the above clay was observed at concentration 8 phr. On the other hand, the increase of Cloisite 20A improves the tensile strength, especially at higher loadings. Similar behavior regarding the effect of clay content on the tensile strength was observed in PDMS hybrids of higher molecular weight, as shown in Figure 4. It can also be observed that tensile strength is affected by the molecular weight of the elastomer but in a different way for the different types of clay reinforcement. In the case of Cloisite 20A, higher molecular weight PDMS matrices give organoclay nanocomposites with lower tensile strength, whereas the opposite effect was recorded for Cloisite 30B/PDMS nanocomposites.

The incorporation of OMMT, in both types of PDMS, results in an increase of modulus of elasticity, but this effect is rather modest compared to that recorded for tensile strength, as can be seen from Figure 5. In the case of low-molecular weight PDMS systems, Cloisite 20A nanocomposites show higher modulus in comparison with that of systems containing Cloisite 30B. Regarding the nanocomposites

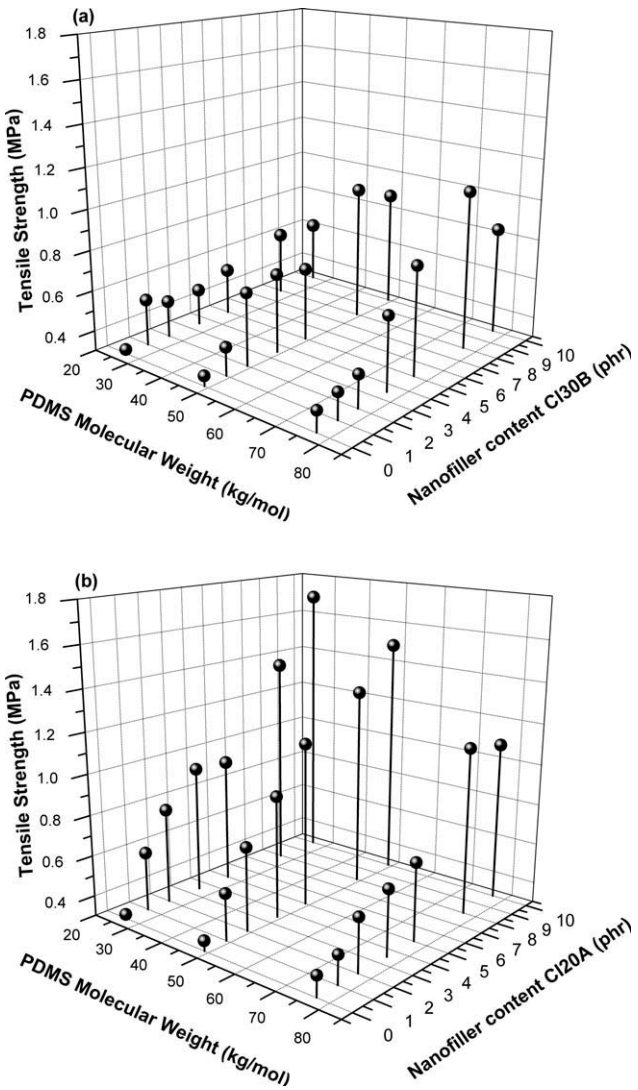

Figure 4 Tensile strength versus PDMS molecular weight and nanofiller content for (a) Cloisite® 30B/PDMS and (b) Cloisite® 20A/PDMS nanocomposites.

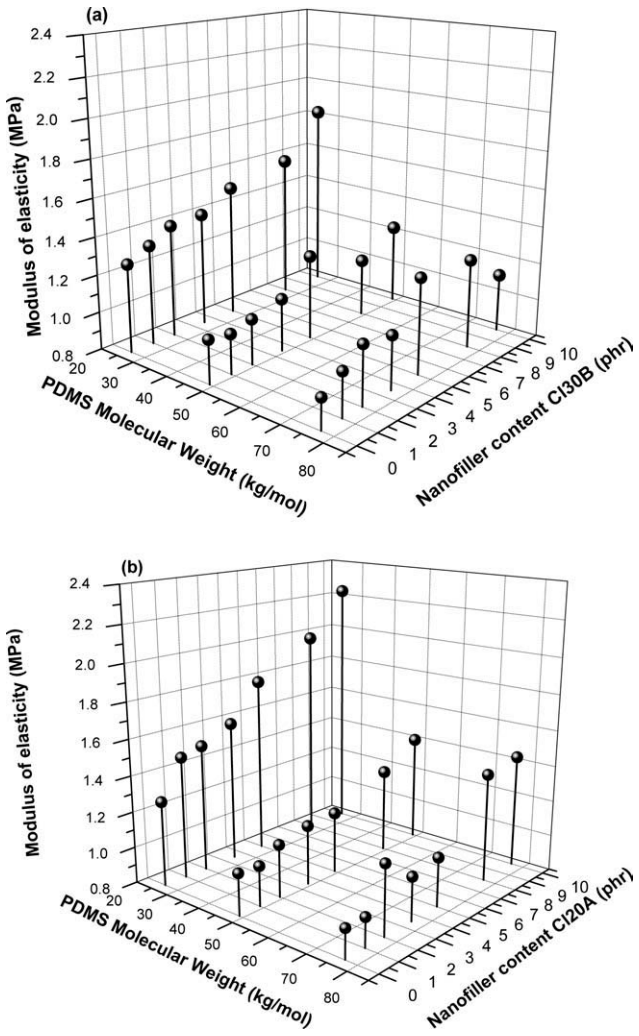

Figure 5 Modulus of elasticity versus PDMS molecular weight and nanofiller content for (a) Cloisite® 30B/PDMS and (b) Cloisite® 20A/PDMS nanocomposites.

of higher molecular weight PDMS, both the above clays resulted in similar improvement of modulus. It was also observed that higher cross-linking density of low-molecular weight PDMS networks leads to higher values of modulus when compared with medium and high-molecular weight systems. This effect may be related with cross-linking density and with the extent of clay intercalation in higher molecular weight PDMS/organoclay hybrids.

As expected, the data obtained for the modulus of elasticity can be directly correlated to the results of hardness, presented in Table II.

From Table III, it can be observed that low-molecular weight pure PDMS gives lower elongation at break in comparison with the higher molecular weight hybrids, which is consistent with the anticipated higher cross-linking density of the former type of elastomer. The incorporation of clay increases the elongation at break of the prepared nanocomposites, especially in the case of medium and high-molecular weight PDMS systems.

From the obtained results, it can be concluded that tensile strength of condensation-type PDMS nanocomposites is more sensitive to the concentration of clay and is influenced by the extent of clay exfoliation in the polymer matrix. As far as the modulus of elasticity of PDMS hybrids is concerned, it is not only influenced by the extent of clay exfoliation but also by the cross-linking density, due to chemical or physical interactions among the system's components.

Tearing is another critical test suitable to allow prediction of the performance of silicone elastomers in biomedical applications, where similar types of loading can take place. The results obtained for the systems studied in this work are presented in Figure 6. Nanocomposites of low-molecular weight PDMS display higher tear strength in comparison with the hybrids of higher molecular weight. Nanocomposites containing Cloisite 20A showed superior properties in comparison with those of Cloisite 30B for both examined PDMS systems. This could be attributed to the better dispersion of Cloisite 20A in the low-molecular weight PDMS matrix and the subsequent intercalation of PDMS molecules in Cloisite 20A silicate layers, as revealed with XRD experiments [Fig. 3].

Simon et al.[25] studied the mechanical properties of silicone nanocomposites with two different types of clay, but they did not find any significant increase in tensile strength and elongation at break. Similar studies found remarkable improvement of

TABLE III
Strain at Break (%) During Tensile Test of OMMT/PDMS Nanocomposites

Clay content (phr)	LMW PDMS		MMW PDMS		HMW PDMS	
	Cloisite 30B	Cloisite 20A	Cloisite 30B	Cloisite 20A	Cloisite 30B	Cloisite 20A
0	35.90 ±9.53		50.99 ±17.31		80.84 ±17.16	
1	56.16 ±11.27	63.57 ±20.32	102.98 ±20.03	111.77 ±16.88	93.21 ±27.97	101.65 ±21.27
2	54.50 ±15.19	79.57 ±14.13	135.23 ±29.97	154.78 ±22.87	110.48 ±12.16	128.35 ±21.81
3.5	51.20 ±12.72	85.71 ±12.00	139.53 ±18.09	176.86 ±13.73	143.35 ±16.63	128.66 ±18.65
5	54.45 ±8.96	70.72 ±17.96	149.99 ±21.50	183.84 ±12.74	164.22 ±5.69	124.45 ±17.03
8	58.37 ±18.72	86.72 ±15.84	186.31 ±23.15	200.33 ±5.20	175.25 ±23.81	177.88 ±20.55
10	50.55 ±15.89	97.03 ±7.94	171.19 ±18.25	218.56 ±11.28	139.11 ±20.77	146.95 ±38.64

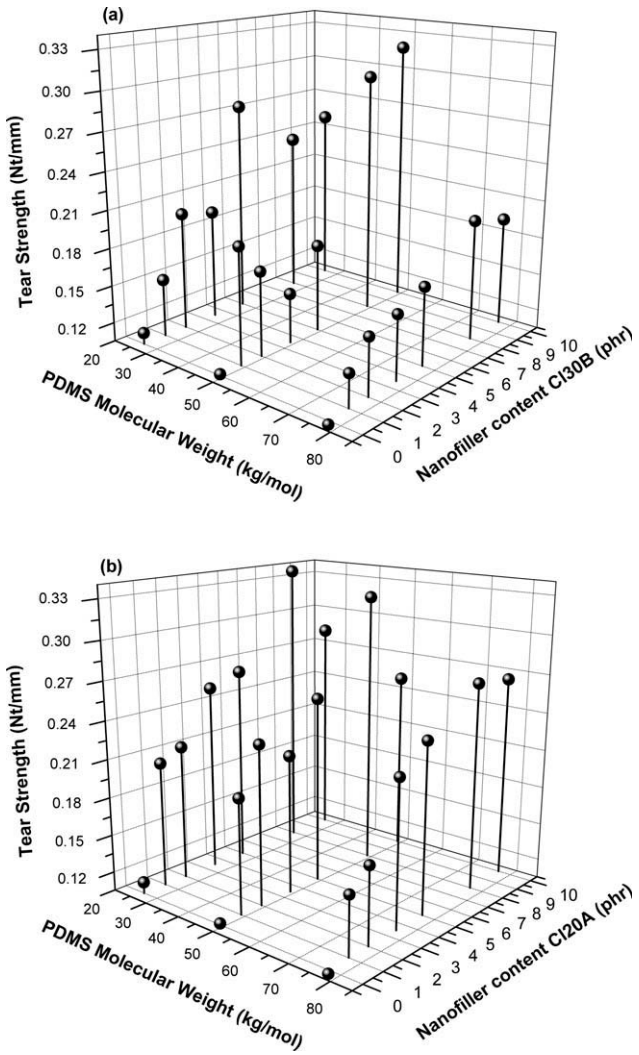

Figure 6 Tear strength versus PDMS molecular weight and nanofiller content for (a) Cloisite® 30B/PDMS and (b) Cloisite® 20A/PDMS nanocomposites.

mechanical properties, due to the introduction of clay and its interaction with silicone matrix.[9,24,26]

Studies on PDMS/montmorillonite systems, carried out by Schmidt and Giannelis,[16] show again a decrease in tensile and tear strength with increasing the base-resin molecular weight, independently of the dispersion state. This suggests the importance of interfacial interactions, obviously related to changes of the end-group concentration.

Swelling experiments in toluene

To correlate the mechanical properties with elastomer structure, swelling experiments were carried out in toluene, as a means of calculation of the network density. As can be seen from Table IV, swelling of reinforced specimens shows a decrease in solvent uptake when compared with that corresponding to unfilled PDMS. The main mechanism that controls solvent uptake is diffusion, which is hindered by the presence of clay particles, as they increase the "tortuosity" path. Furthermore, the interactions between clay particles and silicone molecules may increase the cross-linking density by adding virtual cross-links and, therefore, restrict penetration of the solvent into the matrix. However, each type of OMMT has a different effect on the swelling properties of PDMS matrix.

The effect of polysiloxane molecular weight on toluene uptake, based on weighing measurements, was assessed by the polymer volume fraction in the swollen network (u_2). A plot of polymer fraction u_2 at equilibrium versus PDMS molecular weight and nanofiller content appears in Figure 7. As the molecular weight increases, higher toluene uptake is observed, due to the lower hydroxyl content resulting in decreased cross-linking density. Comparing nanocomposites with the same clay concentration, it is observed that hybrids of Cloisite 20A [Fig. 7(b)] give lower toluene uptake than those of Cloisite 30B [Fig. 7(a)], in all the examined PDMS molecular weights. This behavior could probably be explained by considering the nanocomposite structure, that is, the extent of exfoliation or intercalation of clay in the PDMS matrix. It is expected that more exfoliated structures of Cloisite 20A increase the tortuosity path and, therefore, inhibit diffusion of toluene in the bulk elastomer. In addition to the above, diffusion mechanism is strongly influenced by cross-linking density. Therefore, any interactions of OMMT with the cross-linked structure of the elastomer influence the swelling behavior of the nanocomposite. The results obtained from swelling experiments are in agreement with

TABLE IV
Swelling at Equilibrium by Immersion in Toluene of OMMT/PDMS Nanocomposites

OMMT	Low-molecular weight PDMS		Medium molecular weight PDMS		High-molecular weight PDMS	
Content (phr)	Cloisite 30B	Cloisite 20A	Cloisite 30B	Cloisite 20A	Cloisite 30B	Cloisite 20A
0	196.45 ± 0.40		282.41 ± 0.99		307.64 ± 2.74	
2	185.57 ± 0.92	173.69 ± 0.62	269.12 ± 2.45	249.13 ± 1.96	299.86 ± 1.96	267.60 ± 1.89
5	182.40 ± 0.37	159.15 ± 0.87	252.73 ± 1.74	233.00 ± 1.83	291.49 ± 1.85	254.68 ± 2.19
8	166.13 ± 0.95	156.57 ± 1.07	245.80 ± 1.80	229.45 ± 1.70	247.24 ± 4.53	251.12 ± 1.52

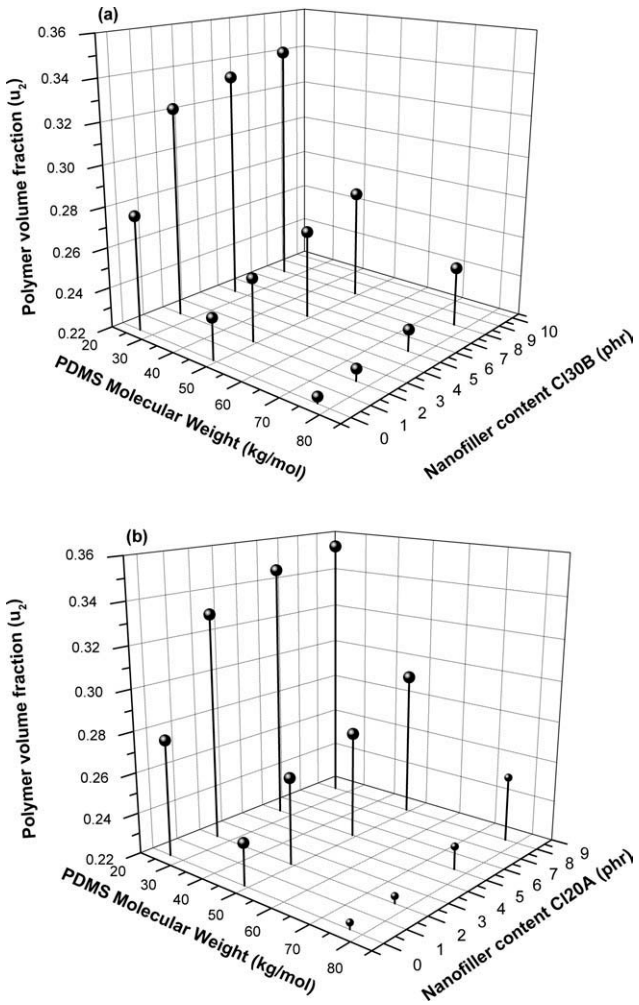

Figure 7 Polymer volume fractions in swollen polymer network at equilibrium versus PDMS molecular weight and nanofiller content for (a) Cloisite® 30B/PDMS and (b) Cloisite® 20A/PDMS nanocomposites.

those of tensile tests, where Cloisite 20A nanocomposite showed superior mechanical properties in comparison with the nanocomposites of Cloisite 30B.

As already stated, for the nanocomposite systems studied in this work, the increased surface area of nanoparticles might promote some interactions with the silicone matrix, and, therefore, it may lead to the formation of additional crosslinks, which can give increased network density to the final product. This leads to the lower amounts of solvent uptake and, thus, to lower swelling of the filled nanocomposite. Similarly, Burnside and Giannelis[1] observed significant decrease of solvent uptake in PDMS-silica nanocomposites when compared with that of intercalated or immiscible hybrids, even at filler concentrations of 1 v/v %. They report that strongly interacting fillers reduce swelling, due to the formation of "bound polymer" in close proximity with the filler, which is either physisorbed or chemisorbed and, therefore, restricts swelling. In a more recent work, the above researchers found that swelling behavior mirrored the amount of bound polymer in the nanocomposite, and they concluded that swelling capacity was controlled by the nanostructure rather than by the increased cross-link density.[27]

Takeuchi and Cohen[8] studied MMT/PDMS nanocomposites and observed that higher modulus and lower swelling in good solvents were obtained only for nonoptimal networks formed with the hydroxyl-terminated precursor chains but not with vinyl-terminated chains. Their results indicate that reinforcement of these elastomers can be attributed to anchoring of hydroxyl end groups to the silicate filler, which dramatically reduces the soluble fraction and binds pendent chain ends.

Table V shows the changes of M_c as a function of clay loadings for low, medium, and high-molecular weight PDMS hybrids. As can be seen, the values of M_c present a tendency to decrease with increasing clay content and decreasing PDMS matrix molecular weight. The results for the cross-linking density of the elastomer obtained via the Flory–Rehner approach are consistent with the changes observed for mechanical properties, and it is confirmed that Cloisite 20A nanocomposites give higher cross-linking density in comparison with Cloisite 30B, due to physicochemical interactions. In addition, for Cloisite 30B/PDMS hybrids, the decrease in cross-linking density, that is, the increase in M_c values, can also be the result of chemical reactions involving the —OH groups of the organic modification. These interactions are expected to consume a certain amount of cross-linker and lead to lower cross-linking density in comparison with that obtained with Cloisite 20A.

TABLE V
M_c (g/mol) Results of OMMT/PDMS Nanocomposites Based on the Flory–Rehner Approach

OMMT	Low-molecular weight PDMS		Medium molecular weight PDMS		High-molecular weight PDMS	
Content (phr)	Cloisite 30B	Cloisite 20A	Cloisite 30B	Cloisite 20A	Cloisite 30B	Cloisite 20A
0	5564.73 ± 21.33		10970.29 ± 71.02		12849.64 ± 125.36	
2	5070.11 ± 62.78	4761.90 ± 43.67	9838.79 ± 133.63	8855.14 ± 129.80	12250.89 ± 542.44	10880.10 ± 189.86
5	4833.68 ± 12.92	4163.01 ± 115.56	8729.49 ± 111.15	8033.41 ± 118.15	11646.64 ± 893.41	10231.77 ± 268.86
8	4365.82 ± 56.29	3895.94 ± 20.01	7744.96 ± 219.17	6691.60 ± 191.64	10063.06 ± 449.93	10122.31 ± 781.07

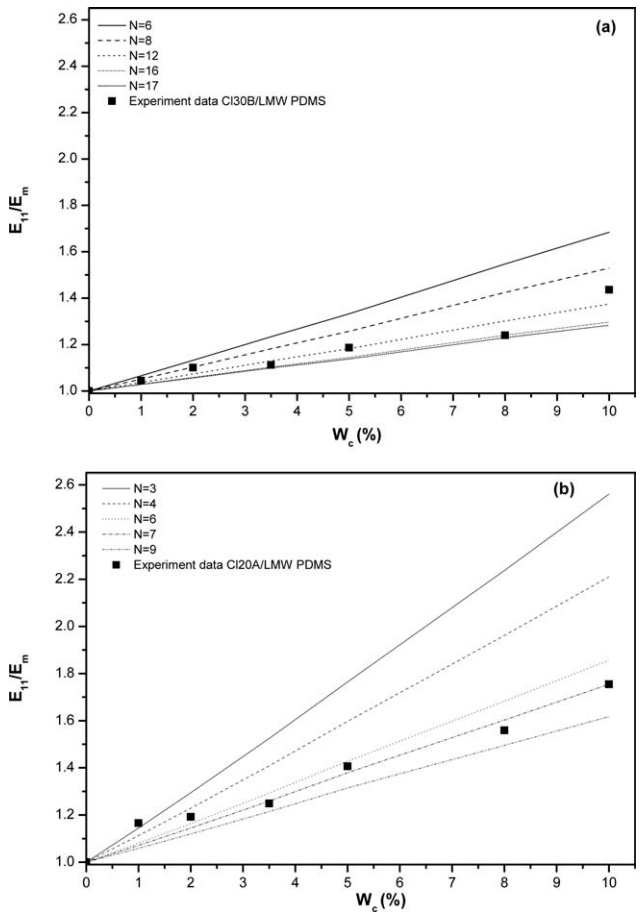

Figure 8 Effect of single silicate sheets (N) on the macroscopic modulus predicted by the Halpin–Tsai model for (a) Cloisite® 30B/LMW PDMS and (b) Cloisite® 20A/LMW PDMS nanocomposites.

Micromechanical modeling

Numerous attempts have been made for modeling the properties of nanocomposites and correlation of the experimental data with the deriving models. In this work, the Halpin–Tsai equations were considered as a tool suitable to predict tensile modulus, as a function of the morphology of MMT/PDMS nanocomposites.[17]

For given values of N, the relation of ratio E_{11}/E_m versus W_p was calculated, and the results deduced from the Halpin–Tsai model were compared to the experimental data for nanocomposites containing Cloisite 30B [Figs. 8(a)–10(a)] and Cloisite 20A [Figs. 8(b)–10(b)]. It is observed that low-clay concentration structures with low number of sheets (N) gave better simulation results, whereas as the clay content increases, N shifts higher, due to poor dispersion within the polymer matrix. By comparing the two types of OMMT, it is confirmed that best dispersion of clay sheets was achieved with Cloisite 20A reinforcement, which is in agreement with the evidence obtained via mechanical testing and swelling experiments.

HMW PDMS nanocomposites show much higher N values (Fig. 10), in comparison with hybrids of lower molecular weight, due to different structures formed in this system. Cloisite 20A clay shows lower N values than Cloisite 30B. These results are in agreement with the XRD data, where more efficient intercalation was achieved in the former type of nanocomposites in comparison with that of Cloisite 30B hybrids.

Halpin–Tsai model assumes that matrix and particles are linear elastic, isotropic, and that a perfect bonding takes place between particles and matrix. It also assumes that there is no agglomeration and interactions among particles and further requires perfectly aligned particles with the displacement load. Neither of these assumptions applies here, as the particles are randomly orientated, and there are interactions among them. So, the number of layers can be slightly greater than that obtained by this

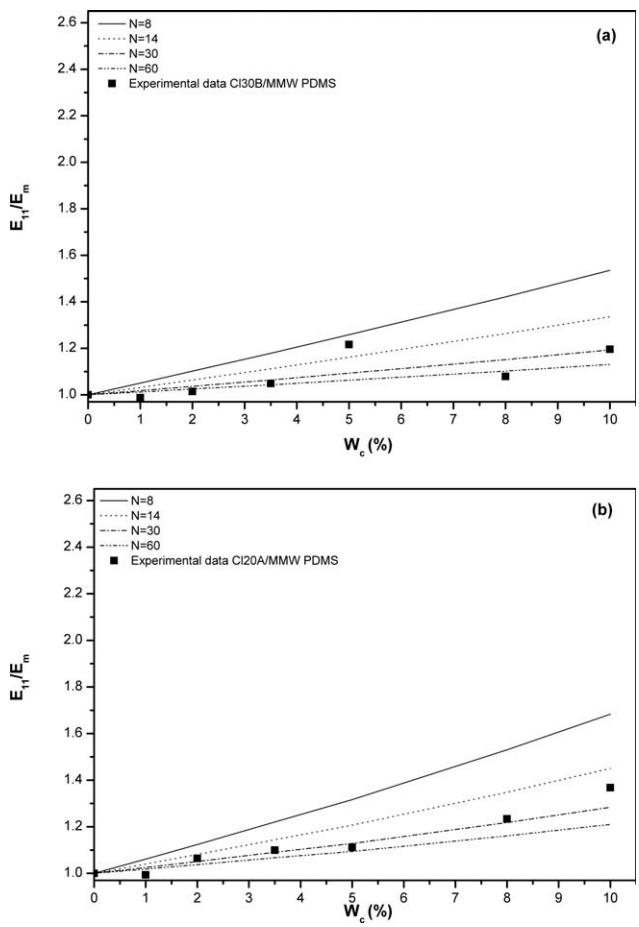

Figure 9 Effect of single silicate sheets (N) on the macroscopic modulus predicted by the Halpin–Tsai model for (a) Cloisite® 30B/MMW PDMS and (b) Cloisite® 20A/MMW PDMS nanocomposites.

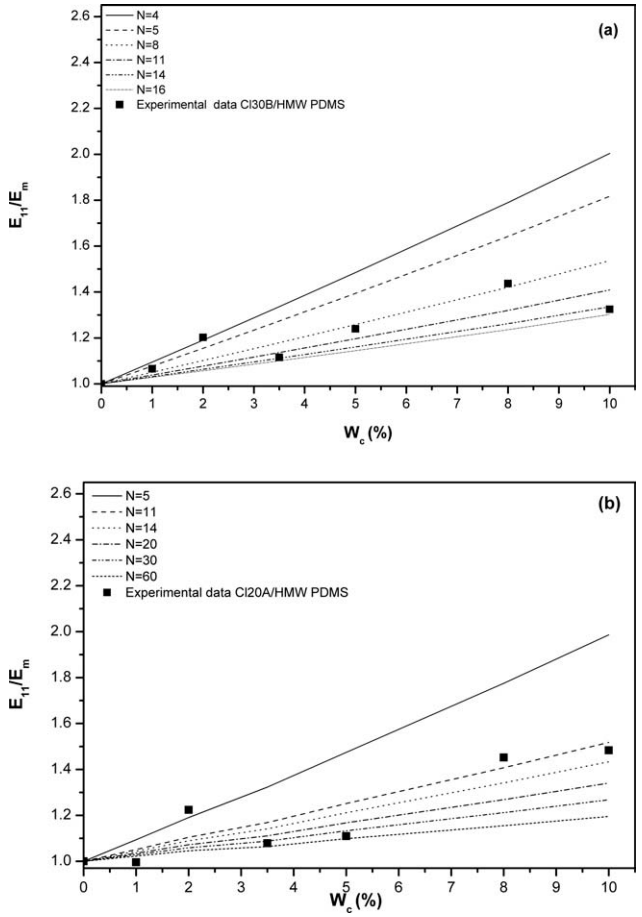

Figure 10 Effect of single silicate sheets (*N*) on the macroscopic modulus predicted by the Halpin–Tsai model for (a) Cloisite® 30B/HMW PDMS and (b) Cloisite® 20A/HMW PDMS nanocomposites.

prediction, especially at higher concentrations of organoclay.

CONCLUSIONS

The study of nanocomposites prepared by sonication of condensation-type polysiloxane/layered silicate systems, based on a variety of polysiloxane molecular weights and different grades of MMT with varying organic modification, led to the following conclusions:

Regarding the structure of the obtained nanocomposites, XRD analysis showed that within the experimental conditions of this work, at OMMT concentrations up to 5 phr, intercalated/exfoliated hybrids can be obtained. Low-molecular weight PDMS, due to its higher content of polar hydroxyl end groups and to the increased chain mobility, facilitates intercalation and dispersion process of silicate layers in the elastomeric matrix.

The incorporation of MMT at concentrations up to 8 phr significantly improves the tensile strength of PDMS matrix. An increase was also observed for the modulus of elasticity and strain at break. The incorporation of Cloisite 20A showed higher reinforcing capacity in PDMS in comparison with Cloisite 30B hybrids, due to the higher content organic modification of the former, resulting in increased interlayer distance of clay platelets and, therefore, facilitating intercalation and further exfoliation processes.

The Halpin–Tsai model adjusted for polymer nanocomposites was applied for the assessment of experimental results of modulus of elasticity versus clay weight fraction. A theoretical prediction of the number of dispersed clay sheets in the intercalated nanocomposites was made via the above model, and it was confirmed that lower number of clay sheets may be expected in the case of nanocomposites reinforced with Cloisite 20A and having low-molecular weight polysiloxane system as matrix. Significant improvement was also observed in the tear strength of PDMS, especially when Cloisite 20A was used as reinforcement.

To explain the observed mechanical performance of PDMS/layered silicate hybrids, data relevant to cross-linking density of the elastomer were obtained through swelling experiments in toluene. Swelling capacity of nanocomposites increases as the molecular weight of PDMS matrix increases. The increase in clay content decreases the degree of swelling, probably due to an inhibition of solvent diffusion caused by the clay particles dispersed within the bulk material. Furthermore, to the above, this behavior can be explained by the increase of cross-linking density because of physicochemical interactions between the organoclay reinforcement and polysiloxane molecules, creating virtual cross-links. Cloisite 20A hybrids gave lower swelling in comparison with the respective nanocomposites of Cloisite 30B. Finally, calculation of molecular weight between crosslinks (M_c) using the Flory–Rehner theory was performed, and the results are in agreement with those obtained from the evaluation of mechanical performance of the nanocomposites. Summing up the main findings of this work, we may conclude that processing characteristics, as well as the overall reinforcing capacity of nanofillers, are greatly dependent on the initial molecular weight of the elastomer, because this parameter controls the resulting network density and concentration of polar end groups.

Special thanks go to Dr. M. Evagelatou for arranging for tear testing at EKEVYL Research Center for Biomaterials, Quality testing laboratories.

References

1. Burnside, S. D.; Giannelis, E. P. Chem Mater 1995, 7, 1597.
2. Wang, S.; Long, C.; Wang, X.; Li, Q.; Qi, Z. J Appl Polym Sci 1998, 69, 1557.

3. Wang, J.; Chen, Y.; Jin, Q. Macromol Chem Phys 2005, 206, 2512.
4. Wang, J.; Chen, Y.; Jin, Q. J Adhes Sci Technol 2006, 20, 261.
5. Kim, E. S.; Shim, J. H.; Jung, S. H.; Joo, J. H.; Yoon, J.-S.; Lee, S. H. Polym Int 2010, 59, 479.
6. Labruyère, C.; Gorrasi, G.; Alexandre, M.; Dubois, Ph. Polymer 2009, 50, 3626.
7. Labruyère, C.; Monteverde, F.; Alexandre, M.; Dubois, Ph. J Nanosci Nanotechnol 2009, 9, 2731.
8. Takeuchi, H.; Cohen, C. Macromolecules 1999, 32, 6792.
9. Bokobza, L. J Appl Polym Sci 2004, 93, 2095.
10. Ma, J.; Yu, Z.-Z.; Kuan, H.-C.; Dasari, A.; Mai, Y.-W. Macromol Rapid Commun 2005, 26, 830.
11. Wang, J.; Chen, Y. J Appl Polym Sci 2008, 107, 2059.
12. Kaneko, M. L. Q. A.; Romero, R. B.; Goncalves, M. C. Eur Polym J 2010, 46, 881.
13. Wang, J.; Chen, Y.; Wang, J. J Appl Polym Sci 2009, 111, 658.
14. Horsch, S.; Serhatkulu, G.; Gulari, E.; Kannan, R. M. Polymer 2006, 47, 7485.
15. Schmidt, D. F.; Clément, F.; Giannelis, E. P. Adv Funct Mater 2006, 16, 417.
16. Schmidt, D. F.; Giannelis, E. P. Chem Mater 2010, 22, 167.
17. Halpin, J. C. J Compos Mater 1969, 3, 732.
18. Sheng, N.; Boyce, M. C.; Parks, D. M.; Rutledge, G. C.; Abes, J. I.; Cohen, R. E. Polymer 2004, 45, 487.
19. Manevitch, O. L.; Rutledge, G. C. J Phys Chem B 2003, 108, 1428.
20. Anthoulis, G. I.; Kontou, E. Polymer 2008, 49, 1934.
21. Luo, J.-J.; Daniel, I. M. Compos Sci Technol 2003, 63, 1607.
22. Vaia, R. A.; Giannelis, E. P. Macromolecules 1997, 30, 7990.
23. Kim, E. S.; Kim, H. S.; Jung, S. H.; Yoon, J. S. J Appl Polym Sci 2007, 103, 2782.
24. LeBaron, P. C.; Pinnavaia, T. J. Chem Mater 2001, 13, 3760.
25. Simon, M. W.; Stafford, K. T.; Ou, D. L. J Inorg Organomet Polym 2008, 18, 364.
26. Kim, E. S.; Shim, J. H.; Jung, S. H.; Joo, J. H.; Yoon, J.-S.; Lee, S. H. Polym Int 2010, 59, 479.
27. Burnside, S. D.; Giannelis, E. P. J Polym Sci B 2000, 38, 1595.